Propeller Design to Improve Flight Dynamics Features and Performance for Coaxial Compound Helicopters

Ye Yuan[1,2] , Renliang Chen*[2], and Douglas Thomson[1]
1. University of Glasgow, Glasgow, United Kingdom
2. National Key Laboratory of Rotorcraft Aeromechanics, Nanjing University of Aeronautics & Astronautics, Nanjing, China

Abstract

The coaxial compound configuration has been proposed as a concept for future high-performance rotorcraft. The co-axial rotor system requires no anti-torque device, while the longitudinal thrust is provided by a propeller. A well-designed propeller can ensure both the performance and the cruise efficiency. The propeller design also influences the flight dynamics of such configuration. To design the propeller parameters of the coaxial compound helicopter, the propeller modelling and design method devised by Adkins and Liebeck is firstly introduced. A flight dynamics model of the coaxial compound helicopter is developed. Trim characteristics, power consumption results, and handling qualities features are calculated with variable propeller parameters at optimum (corresponding to the maximum flight range) and maximum speeds. The results indicate that the propeller parameters alter its efficiency and improve the performance characteristics of this helicopter. In addition, the propeller design also influences the flight dynamics characteristics and handling qualities of the coaxial compound helicopter, and consequently affect the power consumption indirectly. In this light, a design method for the propeller has been developed by formulating the design procedure into the nonlinearly constrained optimisation problem based on the flight dynamics characteristics. The method is demonstrated by evaluating propeller parameters to improve the performance in both optimum and high-speed range, which could also guarantee the handling qualities of the rotorcraft for related requirements.

Nomenclature

C_l, C_D	Local lift and drag coefficient
F	Momentum loss factor
I_β	Blade moment of inertia (kg.m^3)
K_{10}	Rigidity of the equivalent flapping spring (N. m/rad)
L, M, N	Moment components in body axis (N. m)
$M_{a,critical}$	Critical Mach number
M_β	Blade mass static moment (kg.m^2)
N_b	Number of blades
R	Radius (m)
S	Characteristic area of the helicopter part (m^2)
U_p	Axial velocity on the propeller (m/s)
V_f	Freestream velocity (m/s)
W	Local total velocity (m/s)
X, Y, Z	Force components in body axis (N)
a, a'	Axial and rotational interference factor of the propeller
a_c	Local speed of sound (m/s)
c	Chord (m)
$\bar{e}$	Non-dimensional flapping offset
l	Characteristic length of the helicopter part (m)
q	Local dynamic pressure (N/ m^2)
r	Radius position (m)
x, y, z	The position coordinate in body axis (m)
w_t	Tangential velocity component (m/s)
Γ	Circulation (m^2/s^2)
Ω	Rotational speed (rad/s)
α	Angle of attach (rad)
α_{rp}	Factor for the thrust allocation between rotors and propeller
ξ	Non-dimensional induced velocity
ε	Airfoil lift to drag ratio
θ_p	Propeller collective (rad)
$\theta_{pretwist}$	Blade twist angle (rad)
θ_{1s}	Longitudinal cyclic pitch (rad)
$\theta_{I,l}$	Longitudinal control input (rad)
ρ	Air density (kg/m^3)

Subscript

F	Fuselage
ht	Horizontal tail
p	Propeller

R	Rotor
vt	Vertical tail

Introduction

There has been much research into the coaxial compound helicopter in recent years due to its high-speed performance [1, 2] and significant cruise-efficiency [3]. A properly designed propeller is the key to achieve these two important features. With reasonable parameters, the propeller can offload the rotor by producing most of the propulsive forces in flight. It can alleviate the compressibility effect across the advancing side of the rotor disc [4], and consequently reduce the power consumption at the high-speed range. The coaxial compound helicopter can also increase the cruise efficiency with proper design of the propeller parameters by increasing the propeller efficiency at the optimum flight range [5].

Two considerations should be taken into during the propeller design process. Firstly, the design parameters, including radius, propeller rotational speed, number of blades, should be optimised to guarantee the excellent performance in various flight status. Additionally, the position of the propeller plays a major role in the trim, controllability, and stability characteristics. Nevertheless, coupling of propeller parameters and trimming features of the helicopter affects the required power of the coaxial rotors in a more complicated manner [6~9]. Also, the propeller optimisation influences other flight dynamics characteristics, such as the dynamic stability and the inter-axis coupling [10]. Potentially, the careful selection of propeller parameters could be a useful mean to improve the handling qualities of the coaxial compound helicopter.

Fig. 1 The X2TD helicopter

The propeller design process can be partly achieved using the Adkins-Liebeck method [11-15], but this only gives the optimal distribution of chord and pre-twist distribution for a designated thrust at fixed flow-field. In other words, this method cannot guarantee the propeller of the coaxial compound helicopter to have a satisfactory performance across its flight range. The X2TD helicopter (Fig.1) is the first coaxial compound helicopter using an auxiliary propeller to provide extra thrust [16, 17]. For this rotorcraft, the propeller was designed for the best performance at high speed. However, the design methodology for the propeller has not been openly published. Other research on the coaxial compound helicopter [18-21] usually focused on the design and

characteristics of the coaxial rotor and assumed the aerodynamic efficiency of the propeller to be constant. However, Ferguson [22] pointed out that the flight dynamics features and performance are significantly different with various propeller parameters. It can be concluded that during the propeller design process of the coaxial compound helicopter, its flight dynamics characteristics and the power consumption of both the propeller and the coaxial rotors should be considered altogether.

In light of the preceding discussion, this article first introduces the modelling and design method derived from Adkins and Liebeck and presents a flight dynamics model of the coaxial compound helicopter. Validations are made to verify the accuracy of the propeller aerodynamics model and the flight dynamics model. Then the influence of different propeller parameters on the trim, power consumption, the dynamic stability, and the longitudinal to lateral inter-axis coupling is investigated at optimum and maximum speeds. Lastly, this article presents a design method for the propeller to optimise the performance, as well as ensure the coupling handling qualities.

The Adkins and Liebeck Method

The propeller modelling and design method developed by Adkins and Liebeck [15] is summarised here.

Propeller modelling

According to the momentum theory, the thrust per unit dT and the torque per unit dQ can be express as:

$$\frac{dT_p}{dr_p} = 4\pi r_p \rho (1+a) U_p a F \tag{1}$$

$$\frac{1}{r}\frac{dQ_p}{dr_p} = 4\pi r_p^2 \rho (1+a) U_p a' F \Omega_p \tag{2}$$

where a and a' are the axial and rotational interference factor, respectively; F is the momentum loss factor, accounting for radial flow of the fluid. a, a' and F are given by the following equation according to Adkins and Liebeck method:

$$a = (\zeta / 2)\cos^2\phi(1-\varepsilon\tan\phi) \tag{3}$$

$$a' = (\zeta / 2x_p)\cos\phi\sin\phi(1+\varepsilon/\tan\phi) \tag{4}$$

$$F = (\pi/2)\cos^{-1}(e^{-f}) \tag{5}$$

$$f = (N_b/2)(1-\xi)/\sin(\phi_t) \tag{6}$$

$$\tan(\phi_t) = \lambda_p(1+(\xi/2)) \tag{7}$$

$$\tan(\phi) = [U(1+a)]/[\Omega_p r(1-a')] \tag{8}$$

where ζ is the non-dimensional induced velocity distribution of the propeller, which is a function of r_p; x_p is $\Omega_p r_p / U$; λ_p is the speed ratio, x_p is $U_p / \Omega_p R_p$; ξ is the non-dimensional radius. Thus, based on the blade element theory, the propeller thrust and the torque pre unit can then be given by:

$$\frac{dT}{dr} = \frac{dL}{dr}(1-\varepsilon\tan\phi)\cos\phi \tag{9}$$

$$\frac{1}{r}\frac{dQ}{dr} = \frac{dL}{dr}(1+\frac{\varepsilon}{\tan\phi})\sin\phi \tag{10}$$

The angle of attack α can be obtained by:

$$\alpha = \phi - \theta_{pretwist} - \theta_p \tag{11}$$

where θ_p is the propeller collective. The dL and ε are calculated using airfoil aerodynamics look-up table. Thus, with the integration of Eq. (9) and Eq. (10), the thrust T_p and the torque Q_p are obtained. The X_p, Y_p, Z_p forces and the moments L_p, M_p, N_p provided by the propeller can be expressed as:

$$\begin{bmatrix} X_p \\ Y_p \\ Z_p \end{bmatrix} = \begin{bmatrix} T_p \\ 0 \\ 0 \end{bmatrix} \tag{12}$$

$$\begin{bmatrix} L_p \\ M_p \\ N_p \end{bmatrix} = \begin{bmatrix} Q_p \\ Tz_p \\ Ty_p \end{bmatrix} \tag{13}$$

where x_p, y_p, z_p is the Cartesian coordinates of the propeller hub relative to the centre of gravity. In order to verify the accuracy of the proposed propeller calculation method, the related experiment is introduced in this article and the C_T and C_P are compared against the experimental results, as shown Fig.2 ($\beta_{0.75R}$ represents the collective pitch at 0.75R). The detail of the experimental propeller settings and parameters can be found in reference [23].

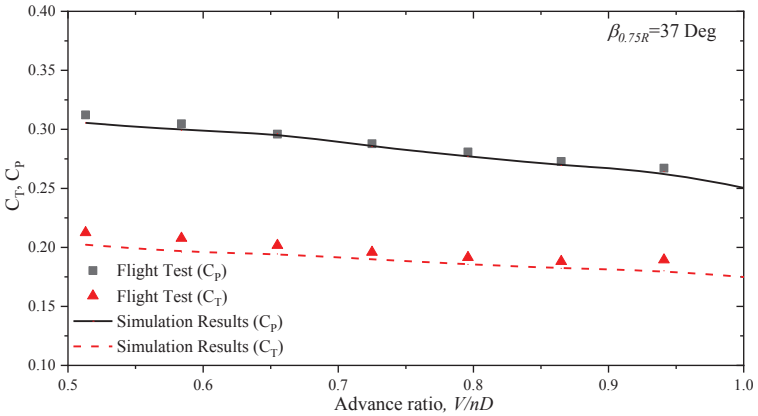

Fig. 2 The propeller aerodynamics validation

As shown in Fig.2, the calculation results are in line with experimental data, indicating the precision of the propeller aerodynamic model, and consequently the flight dynamics analysis and propeller design process can be implemented based on it.

Design method

Using the Adkins-Liebeck method, the pre-twist distribution is obtained using Eq. (11) and the airfoil aerodynamics look-up table. By adjusting the pre-twist distribution, the airfoil is allowed to have the best lift-to-drag ratio at a different radial position.

The chord design is set to maintain the induced velocity, i.e. the circulation Γ, to be constant along with the radial direction to minimise the energy loss of the propeller, which is based on the Betz condition. The determination of the chord distribution needs

the combination of the potential flow theory and the blade element theory. The total lift per unit can be expressed using potential flow theory as:

$$\frac{dT_p}{dr} = N_b \rho W \Gamma \tag{14}$$

$$W = U_p(1+a)/\sin\phi \tag{15}$$

When the induced velocity is constant, Γ is also fixed at various radial positions. Thus, Γ can be expressed using the tangential velocity component w_t in Eq. (16).

$$N_b \Gamma = 2\pi r_p w_t F \tag{16}$$

where w_t can be written using the induced velocity, which is the convective velocity of the wake vortex filament as:

$$w_t = U_p \zeta \sin\phi \cos\phi \tag{17}$$

Thus, the circulation of Eq. (16) can be written as:

$$\Gamma = 2\pi U_p^2 \zeta G / N_b \Omega_p \tag{18}$$

$$G = Fx \cos\phi \sin\phi \tag{19}$$

Also, the total lift per unit can be expressed using blade element theory as Eq. (20):

$$\frac{dT_p}{dr} = N_b \rho W^2 c C_l / 2 \tag{20}$$

where c is the chord; C_l is the local lift coefficient. Thus, c can be expressed in Eq. (21).

$$c = 4\pi\lambda G U R_p \zeta / (C_l N_b W) \tag{21}$$

According to the analysis above, the optimum chord and pre-twist distribution can be directly solved for given inflow states. However, changes of propeller parameters, including the blade chord and the blade airfoil, may lead to additional alteration in the trim results, and stability and controllability of the coaxial compound helicopter, which, in turn, further changes the overall power consumption results at various flight conditions.

Modelling of Coaxial Compound Helicopter

In the present a coaxial compound helicopter model, the external forces and moments are composed of four parts: propeller, coaxial rotor, horizontal and vertical tails, and fuselage. The propeller model has already been introduced in previous sections.

Rotor

The rotor model contains three parts: the induced velocity, the flapping motion, and the aerodynamics load calculation.

This article utilises the Multi-Vortex Ring Element (MVRE) model to calculate the induced velocity of the coaxial rotor. This method is based on the classical fixed wake model and the rotor disc hypothesis. Details of this wake modelling method can be found in reference [24]. Using this model, both the aerodynamic interference between wakes and the wake effect of one rotor on the inflow of the other are calculated. Meanwhile, this rotor wake model is used to calculate the wake-induced velocity on the propeller, which could be used to take the aerodynamic interference between the rotor and the propeller in the flight dynamics model.

The coaxial compound helicopter usually uses ABC (Advancing Blade Concept) rotor to improve the efficiency of the rotor, which has higher flapping rigidity and flapping frequency. Therefore, this paper utilises the equivalence method of equivalent flapping offset and flapping spring [25, 26] to simulate the flapping motion of ABC rotor. The non-dimensional flapping offset $\bar{e}$ can be obtained by:

$$\bar{e} = 1 - \frac{W_{tip}}{R \cdot W'_{0.75}} \tag{22}$$

where W_{tip} is flapping amplitude at the blade tip; $W'_{0.75}$ is the flapping angle at 0.75R. The rigidity of equivalent flapping spring is obtained by Eq. (23) to guarantee the flapping frequency.

$$K_{10} = (\bar{\omega}_n^2 - 1 - \frac{\bar{e} R M_\beta}{I_\beta}) I_\beta \Omega^2 \tag{23}$$

where $\bar{\omega}_n$ is the non-dimension first-order flapping frequency of rigid blade; K_{10} is the rigidity of the equivalent flapping spring.

The calculation of aerodynamics is similar to conventional method [9, 27]. The airfoil section is calculated according to the airfoil aerodynamics look-up table.

Horizontal & Vertical Tails

A simple 2-D representation of the horizontal and vertical tails using conventional strip theory is incorporated into the proposed model. The lift and drag coefficients can be obtained from a 2-D airfoil aerodynamics look-up table. The wake interference on the tails is obtained from the MVRE wake model, with which the wake induced velocity on the tail planes is obtained. Therefore, the dynamic pressure, the force, and the moment of horizontal and vertical tails can be represented in Eqns. (24~29).

$$q_{ht} = 0.5 \rho v_{ht}^2 \tag{24}$$

$$q_{vt} = 0.5 \rho v_{vt}^2 \tag{25}$$

$$\begin{bmatrix} X_{ht} \\ Y_{ht} \\ Z_{ht} \end{bmatrix} = \begin{bmatrix} \cos\beta_{ht} \cos\alpha_{ht} & -\sin\beta_{ht} \cos\alpha_{ht} & -\sin\alpha_{ht} \\ \sin\beta_{ht} & \cos\beta_{ht} & 0 \\ \cos\beta_{ht} \sin\alpha_{ht} & -\sin\beta_{ht} \sin\alpha_{ht} & \cos\alpha_{ht} \end{bmatrix} \bullet \begin{bmatrix} -q_{ht} S_{ht} C_{D,ht} \\ 0 \\ -q_{ht} S_{ht} C_{L,ht} \end{bmatrix} \tag{26}$$

$$\begin{bmatrix} X_{vt} \\ Y_{vt} \\ Z_{vt} \end{bmatrix} = \begin{bmatrix} \cos\beta_{vt} \cos\alpha_{vt} & -\sin\alpha_{vt} & -\sin\beta_{vt} \cos\alpha_{vt} \\ \cos\beta_{vt} \sin\alpha_{vt} & \cos\alpha_{vt} & -\sin\beta_{vt} \sin\alpha_{vt} \\ \sin\beta_{vt} & 0 & \cos\beta_{vt} \end{bmatrix} \bullet \begin{bmatrix} -q_{vt} S_{vt} C_{D,\ vt} \\ -q_{vt} S_{vt} C_{L,vt} \\ 0 \end{bmatrix} \tag{27}$$

$$\begin{bmatrix} L_{ht} \\ M_{ht} \\ N_{ht} \end{bmatrix} = \begin{bmatrix} y_{ht} Z_{ht} - z_{ht} Y_{ht} \\ z_{ht} X_{ht} - x_{ht} Z_{ht} \\ x_{ht} Y_{ht} - y_{ht} X_{ht} \end{bmatrix} \tag{28}$$

$$\begin{bmatrix} L_{vt} \\ M_{vt} \\ N_{vt} \end{bmatrix} = \begin{bmatrix} y_{vt}Z_{vt} - z_{vt}Y_{vt} \\ z_{vt}X_{vt} - x_{vt}Z_{vt} \\ x_{vt}Y_{vt} - y_{vt}X_{vt} \end{bmatrix} \tag{29}$$

where α_{ht} , α_{vt} are the attack angles of the horizontal and vertical tails. β_{ht}, β_{vt} are the sideslip angle of the horizontal and vertical tails, which are decided by the free-stream inflow and wake induced velocity obtained from MVRE model. q is the dynamic pressure. S_{ht}, S_{vt} are the characteristic areas of the horizontal and vertical tails.

Fuselage

The fuselage model is based on the wind tunnel test. Using MVRE wake model, the wake induced velocity on the centre of the fuselage is obtained, and the rotor wake effect on the fuselage is introduced into the flight dynamics model. The force and moment provided by the fuselage are obtained by Eqns. (30) and (31).

$$\begin{bmatrix} X_F \\ Y_F \\ Z_F \end{bmatrix} = \begin{bmatrix} -q_F S_F C_{DF} \\ -q_F S_F C_{YF} \\ -q_F S_F C_{LF} \end{bmatrix} \tag{30}$$

$$\begin{bmatrix} L_F \\ M_F \\ N_F \end{bmatrix} = \begin{bmatrix} q_F S_F l_F C_{RF} \\ q_F S_F l_F C_{MF} \\ q_F S_F l_F C_{NF} \end{bmatrix} \tag{31}$$

where S_F is the sectional area of the fuselage; l_F is the fuselage length; $C_{DF}, C_{YF}, C_{RF}, C_{LF}, C_{MF}, C_{NF}$ are the drag force, lateral force, lift force, rolling moment, pitching moment and heading moment coefficients, obtained from wind tunnel experiments. [28]

Validation

The model is verified by comparing the trim results with flight simulation data found in reference [22] due to the lack of experiment data. The helicopter used in reference [22] is based on the XH-59A helicopter and its primary data is shown in Table.1. It should be mentioned that the XH-59A helicopter utilises two turbojet engines, rather than the propeller, to provide the thrust in high speed flight. Therefore, the data of the propeller in the validation part is derived from reference [22].

Table. 1 The coaxial compound helicopter parameters

Parameter	Value
Rotor radius/m	5.49
Number of blades	3×2
Pre-twist/ (°)	-10
Rotor rotational speed/(rad/s)	35.9
Taper ratio	0.5
Flapping frequency/Ω	1.4
Shaft spacing/m	0.77
Horizontal tail area/m^2	5.57

Vertical tail area/m^2	2.79
Take-off mass/kg	5500
Lower rotor position/m	(0.00,0.00,-0.89)
Centre of gravity/m	(0.00,0.00,0.00)
Horizontal tail position/m	(-6.80,0.00,0.20)
Vertical tail position/m	(-6.80,0.00,-0.50)
Propeller radius/m	1.3
Number of propeller blade	5
Propeller rotational speed/(rad/s)	162
Propeller chord length	0.16
Negative pre-twist/°	-30
Position/m	(-7.66,0.00,0.00)

The trim strategy of the coaxial compound helicopter is unique due to three additional redundant control inputs, the propeller control strategy (propeller collective), the rotor rotational speed, and the lift-offset strategy.

In high speed flight, the rotor rotational speed must reduce to minimise the compressibility effects at the advancing blade tip regions. The rotor rotational speed changes following Eq. (32), which is based on the related study [4].

$$\Omega = \begin{cases} 35.9, V_{\mathrm{f}} < 70\mathrm{m/s} \\ 35.9 - \dfrac{3.59(V_{\mathrm{f}}\text{-}70)}{30}, V_{\mathrm{f}} \geq 70\mathrm{m/s} \end{cases} \tag{32}$$

The Lift-offset (LOS) has a marked impact on rotor aerodynamic efficiency [29~32]. A coaxial rotor with the LOS can attain good efficiency in high-speed flight by operating with more lift on the advancing side than on the retreating side of the rotor disc. In this article, the lateral cyclic pitch differential $\theta_{lc,d}$ is used to further adjust the LOS effect to refine the rotor performance, and $\theta_{lc,d}$ is set to be a trim variable. The LOS is given as Eq. (33), which is according to reference [17].

$$LOS = 0.00002V_f^2 \tag{33}$$

The trim strategy of the propeller collective is aimed to maintain the pitch attitude fixed at a given angle, which is shown in Fig.3 [22]. Therefore, the propeller collective can be set as a trim variable in this investigation.

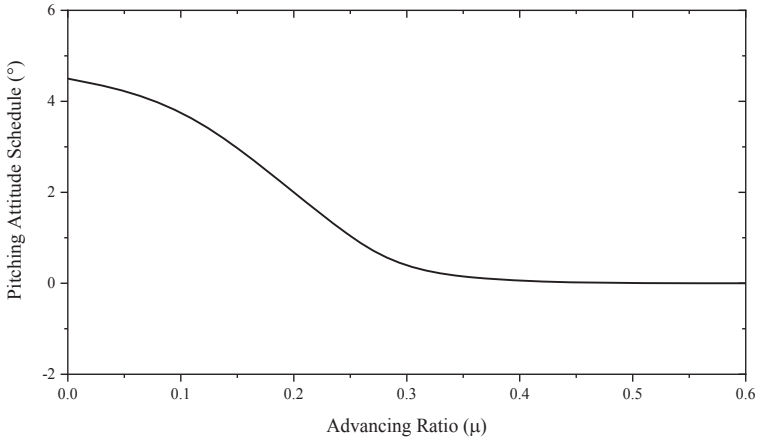

Fig. 3 Pitching Attitude Pre-determined Schedule

Trim comparison results are shown in Fig.4.

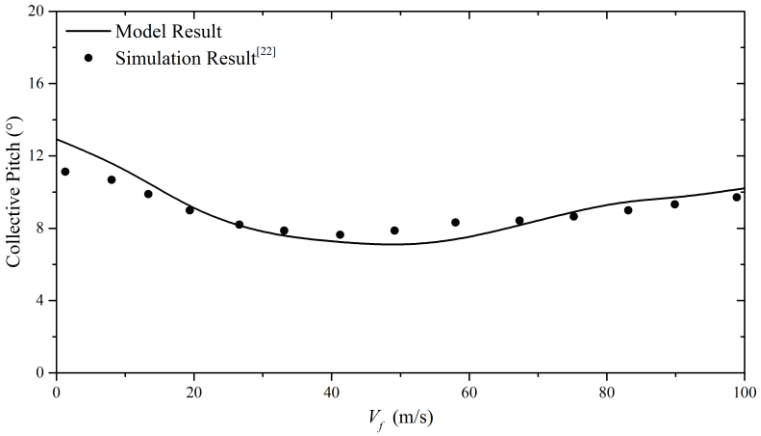

(a) Collective Pitch of Rotor

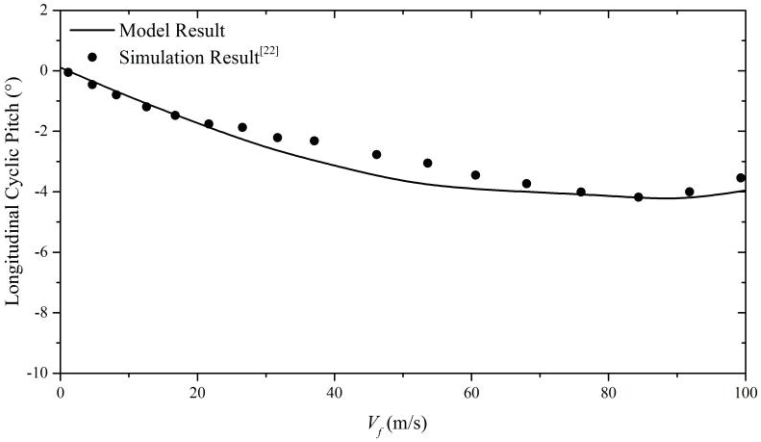

(b) Longitudinal Cyclic Pitch

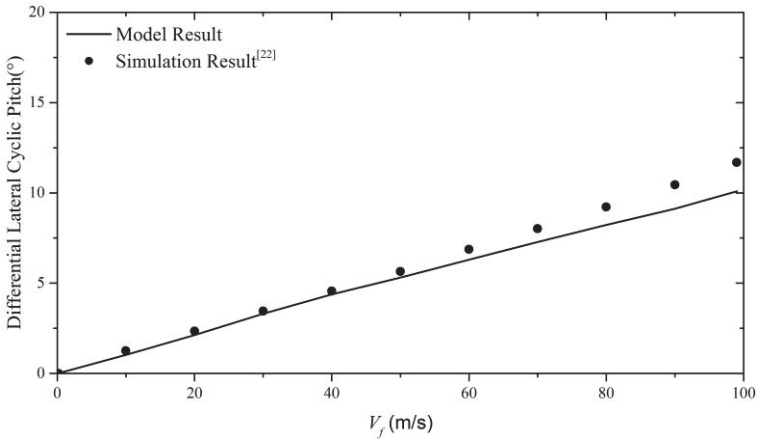

(c) Differential Lateral Cyclic Pitch

Fig. 4 Trim Result Comparison

As demonstrated in Fig. 4, results obtained using this model correlates well with simulation results from other researchers. This gives confidence that the proposed model can be used to analyse the effect of different propeller parameter on the flight dynamic characteristics and performances of the coaxial compound helicopter.

Flight Dynamics & Performance Analysis

The influence of the propeller parameters on the trim characteristics, the power consumption of the propeller and rotor, and the handling qualities including the dynamic stability (eigenvalue) and the inter-axis coupling of roll-rate to pitch-rate (p/q) are analysed. The propeller parameters considered consist of the propeller design parameters and its position with respect to the airframe. The design parameters are normalised using the default value in Table. 1. Besides, the propeller position alters from -1m to +1m concerning the original propeller position coordinate shown in Table.1

The forward speed of 60m/s and 100m/s are set as test points, as they are close to the optimum speed and maximum speed according to the power consumption results given by Ferguson [22]. The improvement of the performance at the optimum and maximum speeds could be beneficial to the helicopter to increase its maximum flight range and high-speed performance, respectively. In order to clarify the coordinate, the schematic diagram of the propeller is shown in Fig. 5. In Fig. 5, $R_{Gr,lim}$ is the limit for the vertical position of the propeller to ensure safety when landing.

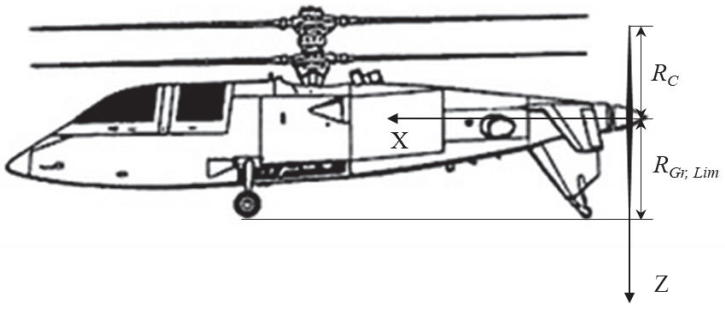

Fig. 5 The schematic diagram of the coaxial compound helicopter propeller

Longitudinal Trim

The longitudinal trim results at 60m/s and 100m/s with various propeller design parameters and the propeller position are shown in Fig.6 and Fig.7, respectively. The

pitch attitude is excluded because it is fixed at a given value according to the trim strategy in Fig. 3.

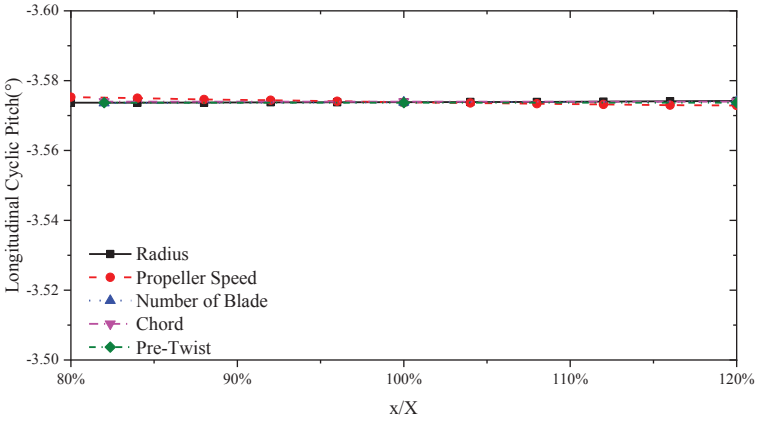

(a) 60m/s: Longitudinal Cyclic Pitch

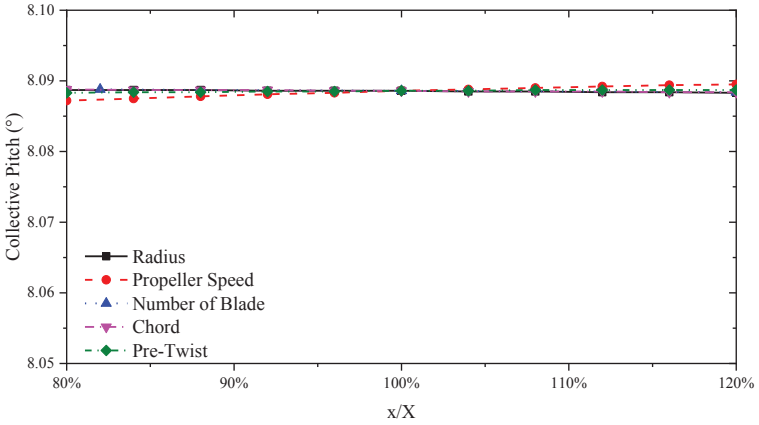

(b) 60m/s: Collective Pitch

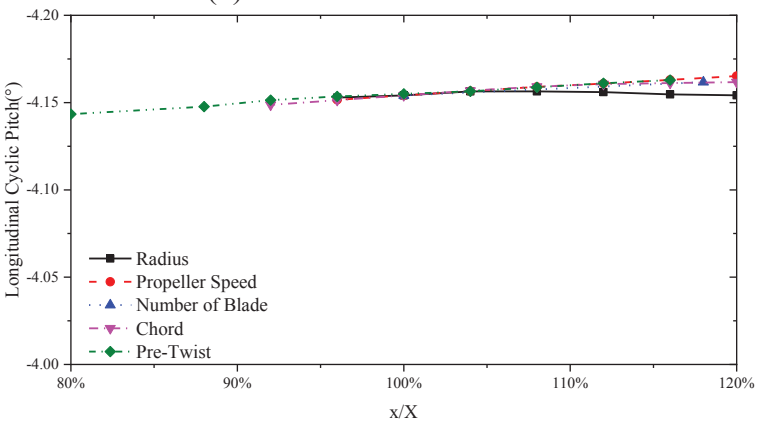

(c) 100m/s: Longitudinal Cyclic Pitch

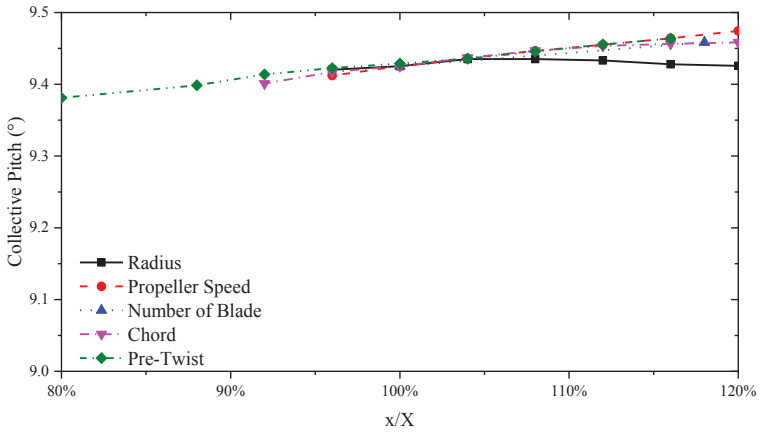

(d) 100m/s: Collective Pitch (°)

Fig. 6 Longitudinal trim with propeller design parameters changing

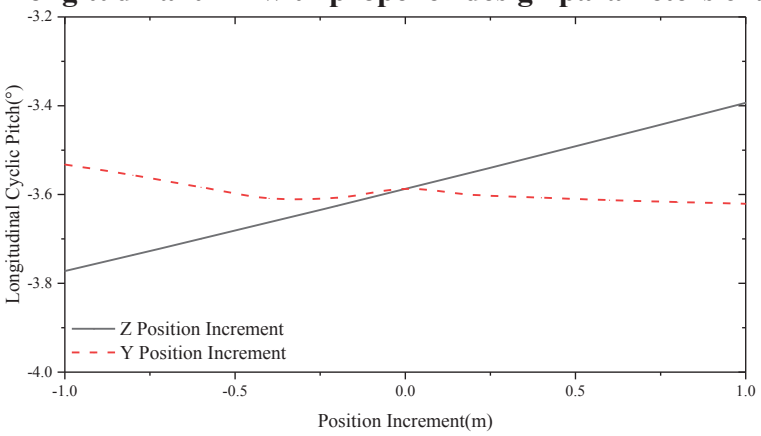

(a) 60m/s: Longitudinal Cyclic Pitch

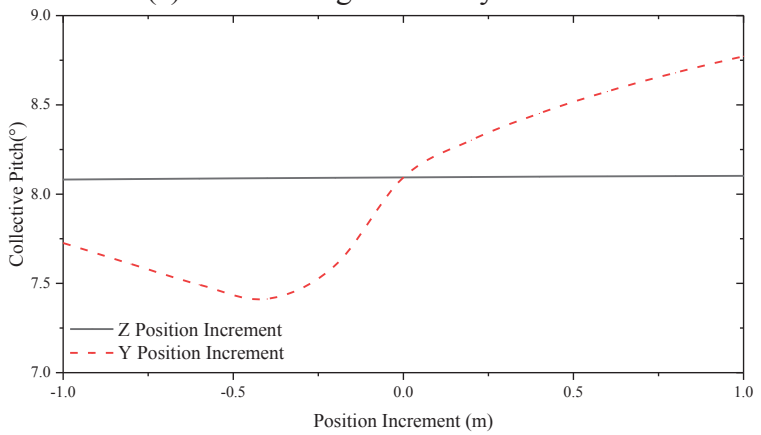

(b) 60m/s: Collective Pitch

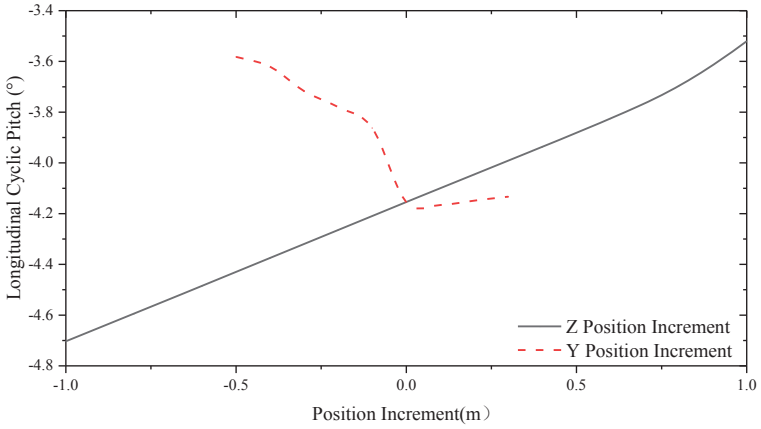

(c) 100m/s: Longitudinal Cyclic Pitch

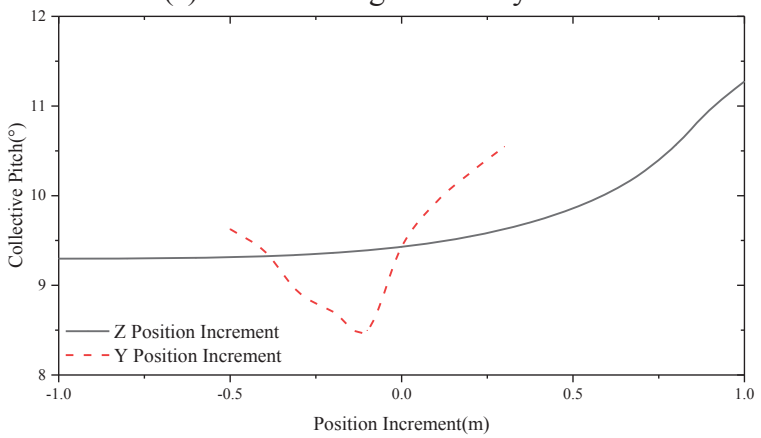

(d) 100m/s: Collective Pitch

Fig. 7 Longitudinal trim with propeller position coordinates changing

As demonstrated in Fig.6, changes of these parameters, e.g. smaller the radii, lower propeller rotational speed, and shorter chord, would cause the helicopter being unable to trim in high speed. As the parasite drag of the fuselage is large at this flight range, the propeller is needed to provide considerable thrust. Reducing these parameters makes the propeller unable to provide enough propulsive force.

The Z position of the propeller has a significant influence on the longitudinal trim characteristics. According to Eqns. (12) and (13), increasing the Z vertical location of the propeller would add nose-down pitch moment to the vehicle, and consequently, the less longitudinal cyclic pitch is required to trim the helicopter. The change of the longitudinal cyclic pitch alters the tilt angle of the rotor tip plane and affects the collective pitch trim results.

The effect of the Y-direction coordinate on the trim results is more complex. The ABC rotor and the lift-offset (LOS) should be considered together to explain this feature. The LOS is defined as:

$$LOS = \frac{M_x}{TR} \tag{34}$$

where M_x is the upper rotor rolling moment. T is the total thrust.

The increase of the Y-direction coordinate of the propeller would provide an extra yaw moment to the helicopter requiring additional collective differential for balancing it. The input of collective differential leads to differences in the lift produced by the lower

and upper rotor, which makes LOS on the lower and upper rotor also different. Therefore, the efficiency of the coaxial rotor changes, which is reflected by the collective pitch trim result. Meanwhile, the collective differential influences the flapping motion and the aerodynamic pitching moment of the upper and lower rotor and alters the longitudinal cyclic pitch trim results.

Lateral Trim

The lateral trim results include the lateral cyclic pitch and the rolling attitude, as shown in Fig.8 and Fig.9 respectively.

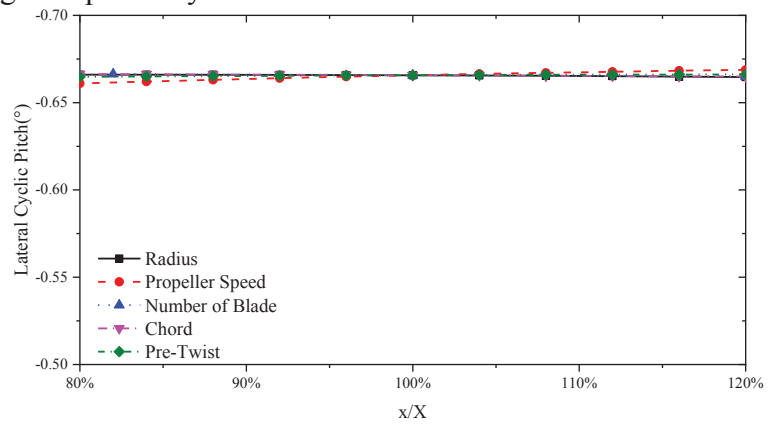

(a) 60m/s: Lateral Cyclic Pitch

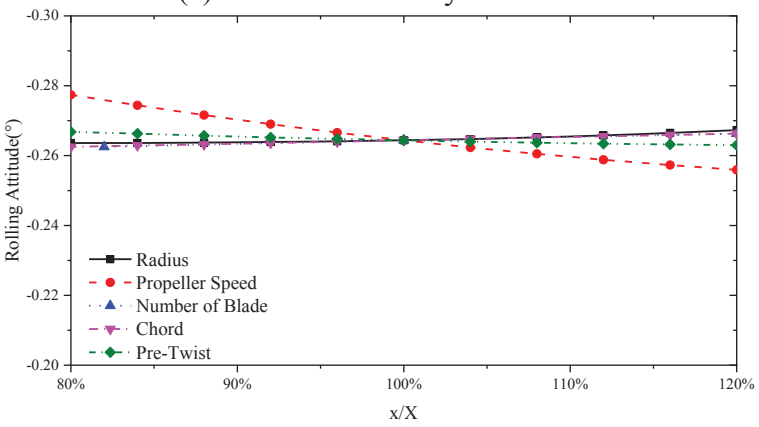

(b) 60m/s: Rolling Attitude

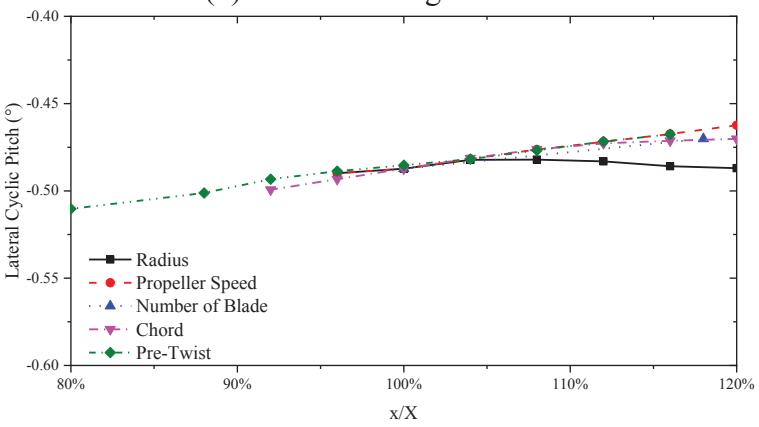

(c) 100m/s: Lateral Cyclic Pitch

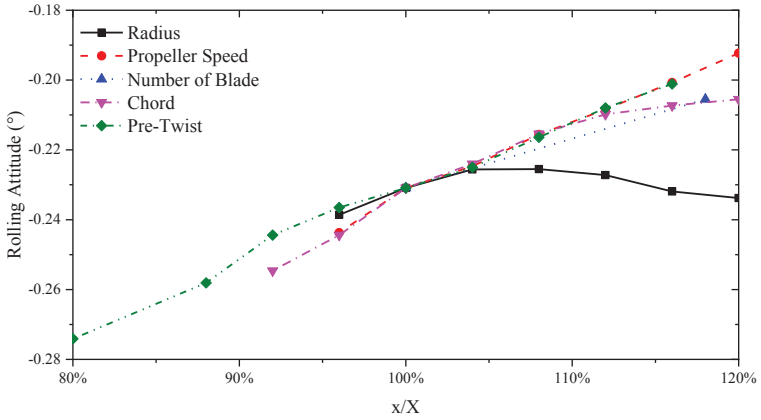

(d) 100m/s: Rolling Attitude

Fig. 8 Lateral Trim Results with Design Propeller Parameters Changing

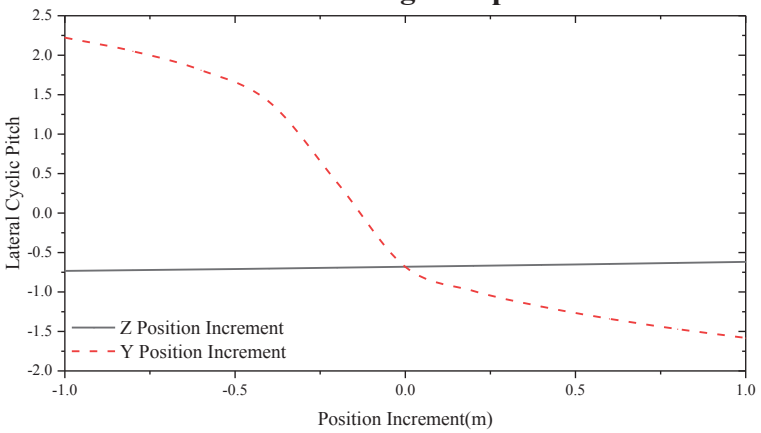

(a) 60m/s: Lateral Cyclic Pitch

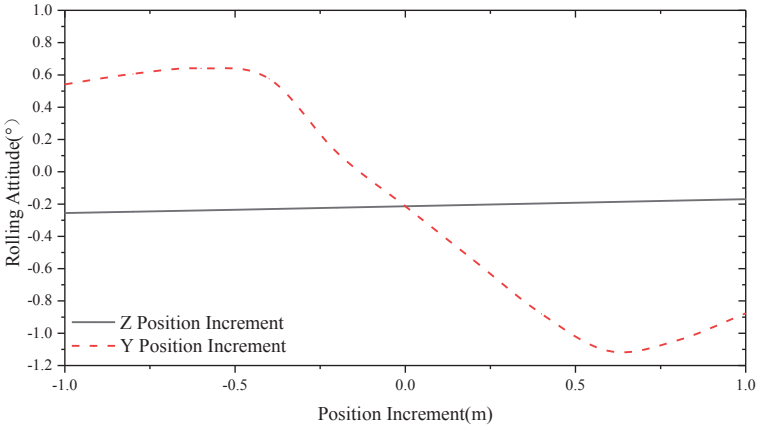

(b) 60m/s: Rolling Attitude

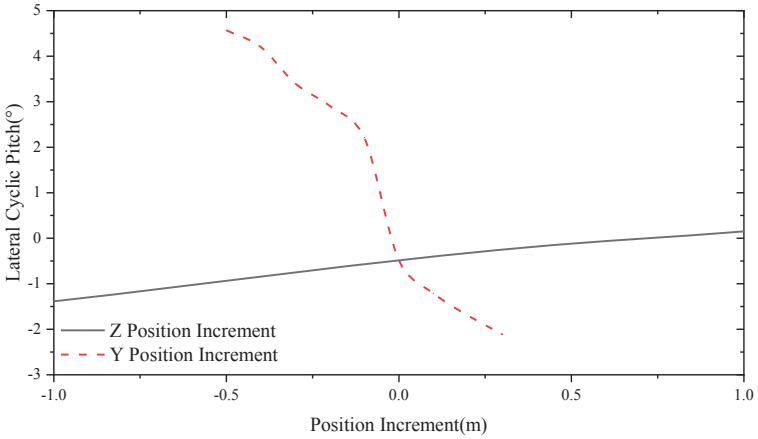

(c) 100m/s: Lateral Cyclic Pitch

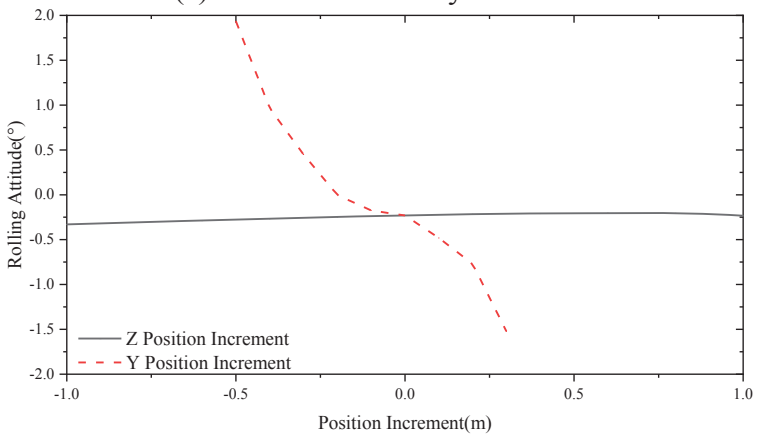

(d) 100m/s: Rolling Attitude

Fig. 9 Lateral Trim Results with propeller position coordinates changing

As indicated in Fig. 8, the design parameters of the propeller influence the lateral trim results. Changes of these parameters alter the torque of the propeller, which in turn provides a rolling moment to the vehicle that increases the rolling attitude and the lateral cyclic pitch. As this torque increases with the forward speed, the effect of the lateral trim results is more obvious when the forward speed is 100m/s.

The Z position of the propeller slightly affects the lateral trim, which is more significant in high-speed flight. The non-dimensional first order flapping frequency decreases at this flight condition due to the rotor rotational speed control strategy [4, 33]. This brings about the inter-axis coupling between longitudinal and lateral controls. Thus, the Z coordinate would change the longitudinal control, which in turn affects the lateral trim results. Moreover, the Z position also alters the torque of the propeller and the lateral trim features.

The Y position significantly influences the lateral trim results, which drives the rolling moment of the upper and lower rotor to be different because of additional collective differential. It needs the lateral cyclic pitch to balance the rolling moment. The rolling attitude follows the alteration of the lateral cyclic pitch because of the high flapping rigidity of the ABC rotor.

It should be mentioned that from Fig. 9 the lateral cyclic pitch would be considerably different if Y position is no longer zero. In this case, the maximum available control input will be reduced to a large extent so that it would be hard for the coaxial compound

helicopter to perform a large amplitude manoeuvre, especially in the lateral channel. Meanwhile, the Y direction change could also introduce additional control coupling between the longitudinal channel and yawing channel. When the pilot applied a propeller control input to accelerate the vehicle, the propeller would also produce an unexpecting yawing moment, requiring the pilot to compensate, increasing workload and reducing the handling qualities rating of the helicopter.

Propeller Collective

The propeller collective trim results with various design propeller parameters and propeller positions are shown in Fig. 10 and Fig. 11, respectively.

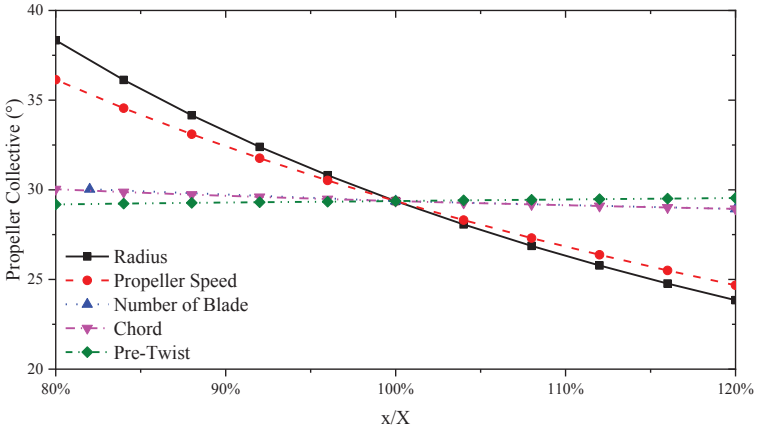

(a) 60m/s

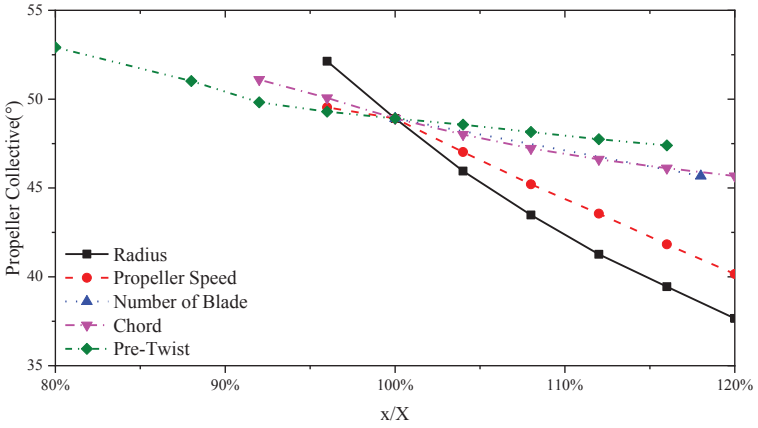

(b) 100m/s

Fig. 10 Propeller Collective with Design Propeller Parameters Changing

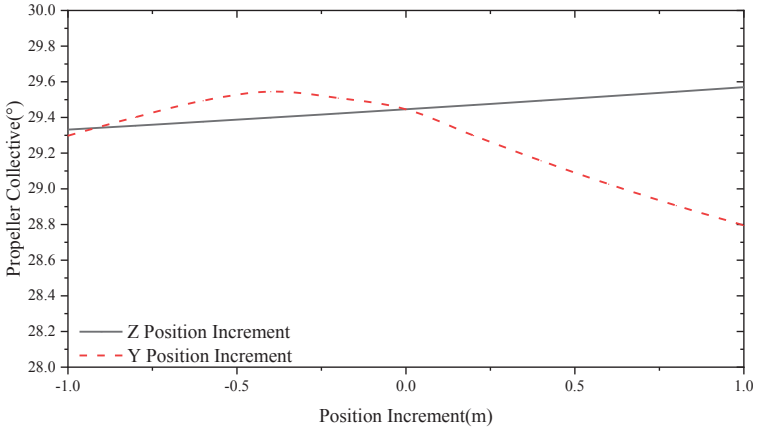

(a) 60m/s

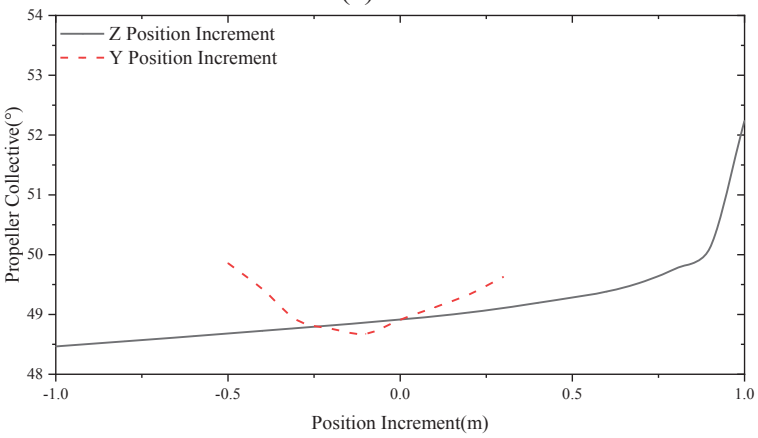

(b) 100m/s

Fig. 11 Propeller Collective with propeller position coordinate changing

The propeller design parameters influence the propeller collective trim results. The increase of the design parameters leads the propeller collective to drop down. This is because the increment of these parameters would introduce additional propeller propulsive force at the given propeller collective. According to Fig. 10, it is noticeable that the change of the pre-twist also alters the propeller collective trim results. This is because the aerodynamic efficiency of the propeller changes along with the pre-twist. Therefore, the alteration of the aerodynamic efficiency would influence the propeller collective trim results.

The Fig. 10 also demonstrates that changes of the propeller collective with propeller design parameters in various speeds are all in the same trend.

As demonstrated earlier, The Z position of the propeller also affects the longitudinal cyclic pitch and pitching attitude, and consequently, the drag of the vehicle is altered. Therefore, the Z position drives the thrust that propeller collective to be different.

The effect of Y position on the propeller collective is different at optimum and high-speed conditions. At the optimum speed range (60 m/s), an Y position increment leads to more longitudinal cyclic pitch as shown above, which drives the main rotors to provide additional thrust. Thus, less thrust is needed from the propeller and consequently reduce propeller collective. In the high-speed flight, the rotor is offloaded, and less thrust can be provided by changing longitudinal cyclic pitch. Meanwhile, the alteration of Y position

causes the parasite drag of the fuselage to increase. Therefore, the propeller collective is lowest when the Y-direction position is around zero at this flight range.

Performance

The power consumption of the propeller and the total vehicle with various propeller design parameters and propeller positions at the speeds of 60m/s and 100m/s are shown in Fig.12 and Fig.13.

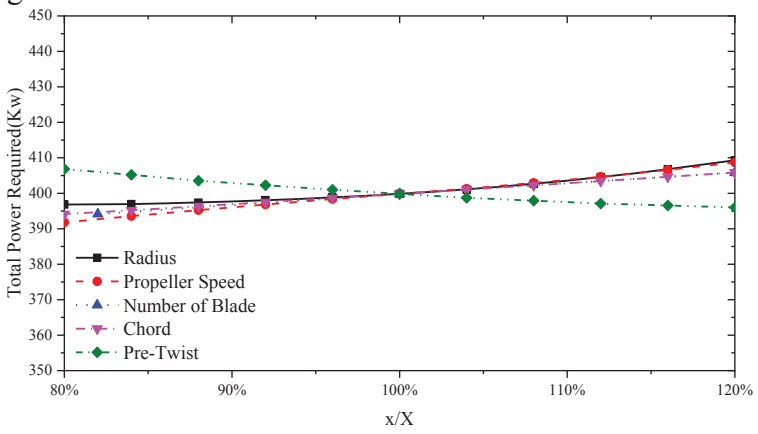

(a) 60m/s: Total Power Required

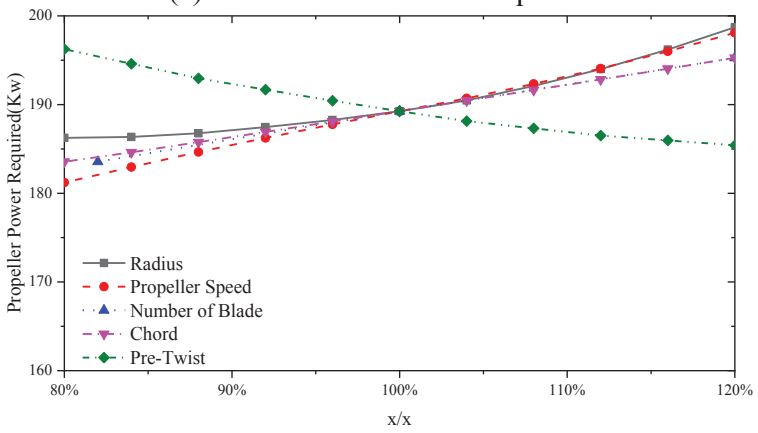

(b) 60m/s: Propeller Power Required

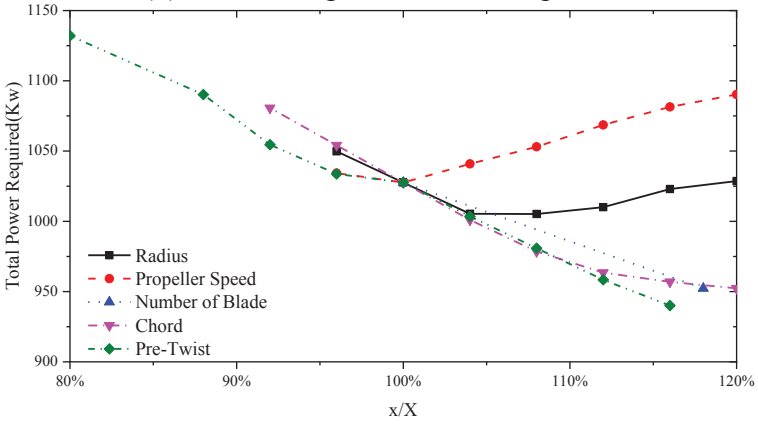

(c) 100m/s: Total Power Required

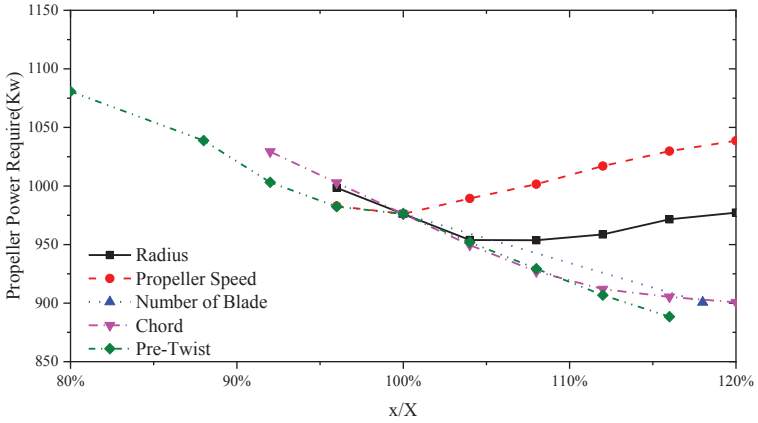

(d) 100m/s: Propeller Power Required

Fig. 12 Power Required with Design propeller parameters

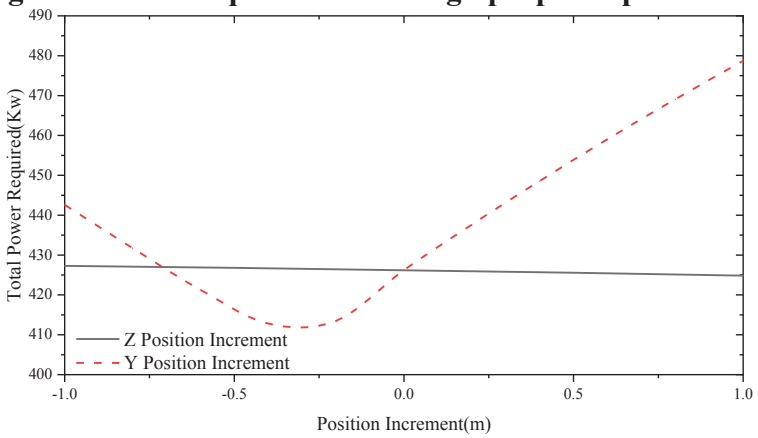

(a) 60m/s: Total Power Required

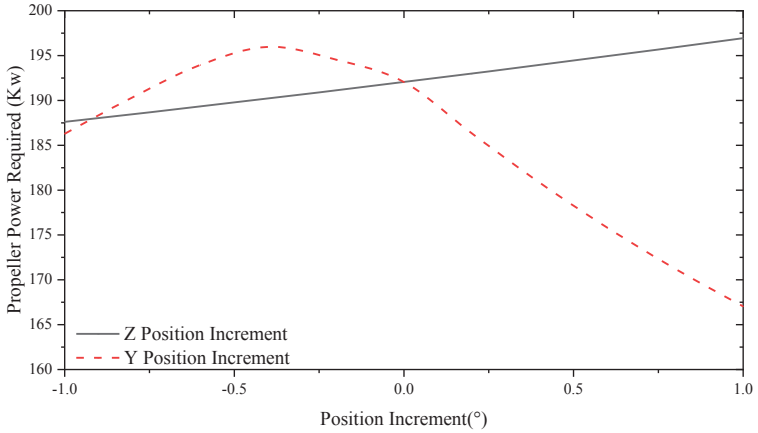

(b) 60m/s: Propeller Power Required

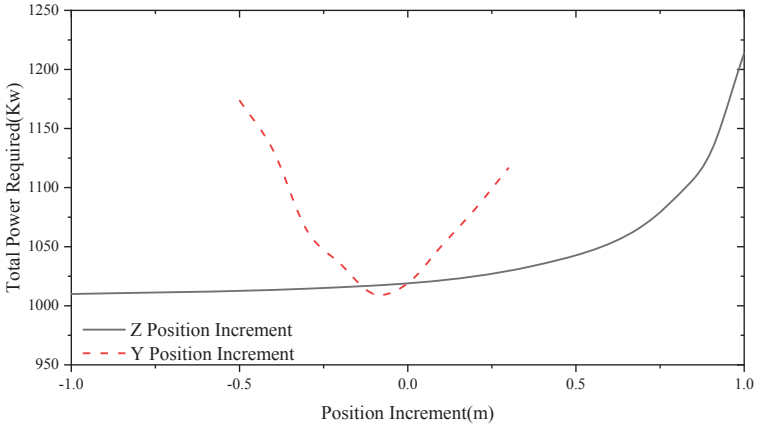

(c) 100m/s: Total Power Required

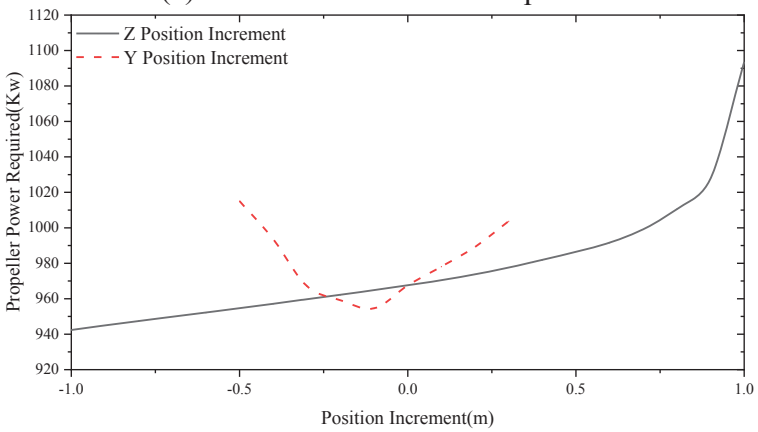

(d) 100m/s: Propeller Power Required

Fig. 13 Power Required with Propeller Position Coordinate Changing

The propeller design parameters mainly alter the power required of the propeller but are not evidently related to the rotor required power. Therefore, when designing the propeller design parameters to reduce the power consumption, it is reasonable to only take the required power of the propeller into consideration.

On the other hand, the position of the propeller affects the power required for both the propeller and the rotor as it significantly influences the trim results of the longitudinal and lateral controls. For example, at the optimum speed range (60 m/s), increasing the Y position reduces the power consumption of the propeller but increase the power of the coaxial rotor, and lead to the increase of the total power required. Thus, the power consumption of both rotor and propeller should be considered in the propeller position design process.

Dynamic Stability

The article utilises the eigenvalue results to assess the effect of the propeller parameters on the dynamic stability. The eigenvalues in longitudinal and lateral with various propeller parameters are shown in Fig. 14 according to the boundaries derived from the ADS-33E-PRF [34] forward flight requirement.

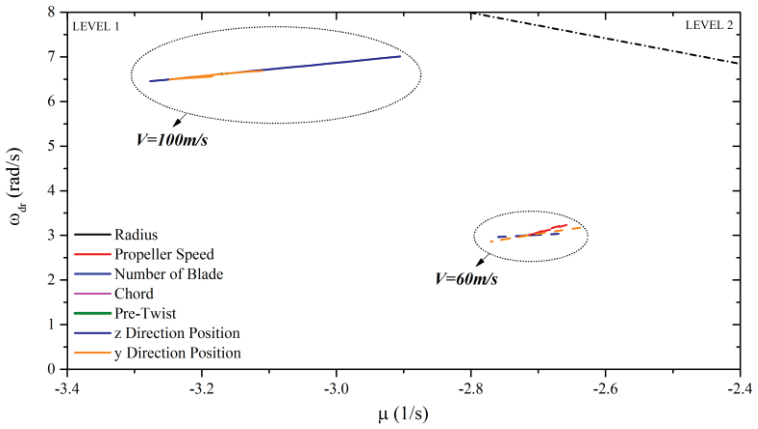

(a) Short-Term Pitch Mode

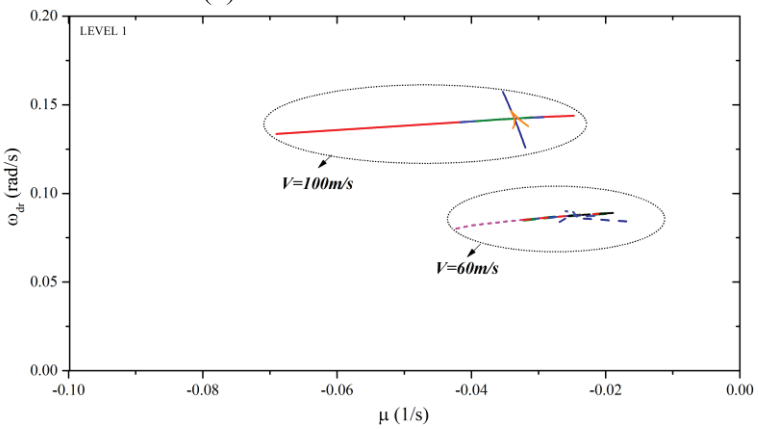

(b) The Longitudinal Mode

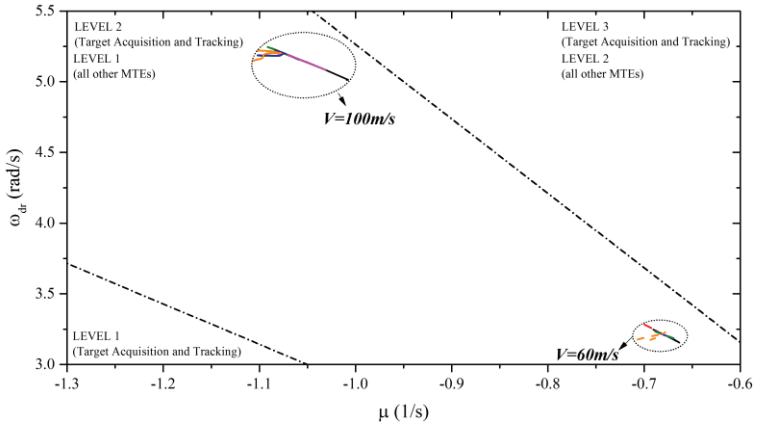

(c) Lateral-Heading Oscillation Mode

Fig. 14 Eigenvalue with Propeller Parameter Changing

As demonstrated in Fig.14, the propeller parameters have a slight influence on the lateral mode eigenvalues and more evident alteration is shown in longitudinal eigenvalue results. The change of the propeller radius, chord, and the number of blades affects the solidity of the propeller, and the propeller rotational speed alters the dynamic pressure on the propeller disc, which leads to additional influence in the forward velocity damping. The Z-direction coordinate of the propeller changes the velocity stability derivative of the helicopter. All these influences the eigenvalue of the longitudinal mode and the short-term pitch mode.

The eigenvalues of the coaxial compound helicopter at optimum and maximum speed range are all in the Level 1 except for the Dutch roll mode in lateral-heading oscillations mode. The coaxial compound helicopter only has vertical tails to provide the lateral stability, and its efficiency is relatively low compared with the tail rotor of the conventional helicopter, which is a unique feature of the coaxial helicopter.

Coupling

The longitudinal to lateral (p/q) inter-axis coupling requirement has a direct relationship with the propeller parameters, and it is also affected by the thrust allocation between rotors and propeller, which can be described by Eq. (35) with the factor a_{rp}.

$$X_P / (X_R + X_P) = a_{rp} \tag{35}$$

The factor a_{rp} could also represent the allocation of the longitudinal control between rotor and propeller, shown in Eq. (36)

$$\Delta\theta_{1,l} = a_{rp}\Delta\theta_p + (1 - a_{rp})\Delta\theta_{1s} \tag{36}$$

Where $\Delta\theta_{1,l}$ is the longitudinal control input increment; $\Delta\theta_p$ is the propeller collective increment; $\Delta\theta_{1s}$ is the increment of the longitudinal cyclic pitch. When the factor a_{rp} is close to 1.0 and the Z-direction coordinate of the propeller is around zero, the longitudinal control input provides relatively large rolling moment and no pitching moment. This leads to severe inter-axis coupling phenomenon. To prevent this disadvantageous situation, the relationship between Z-direction coordinate and the inter-axis coupling is calculated with respect to the related requirement of the ADS-33E-PRF.

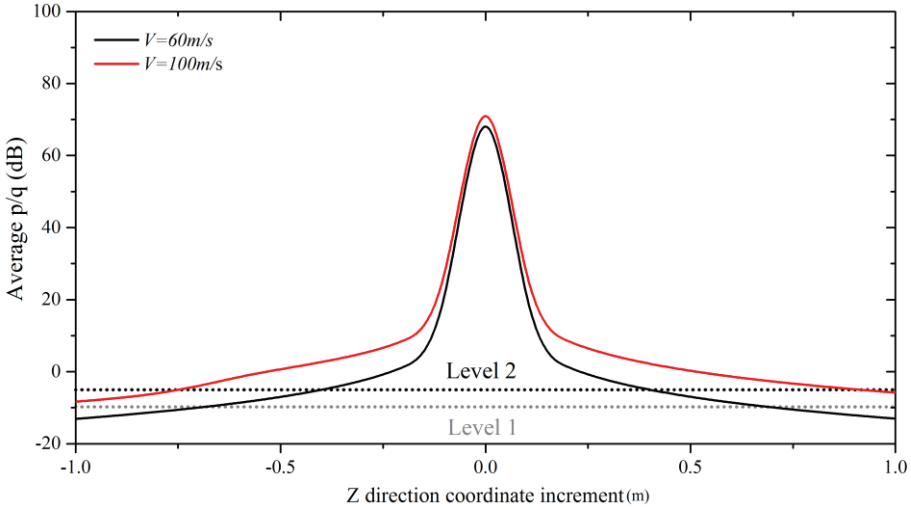

Fig. 15 p/q inter-axis coupling with propeller Z direction changing

As presented in Fig.15, the propeller Z-direction coordinate increment has a significant influence on the average p/q inter-axis coupling. When the coordinate of Z is around zero, the average p/q inter-axis coupling would be quite serious at both optimum and maximum speed ranges, which are rated as Level 3 according to the handling qualities specification. In addition, when the Z coordinate is positive, the direction of the pitching moment is opposite to the pitch moment provided by the longitudinal cyclic pitch, which causes the additional handling qualities problem. Thus, the Z-direction should be optimised to ensure the forward flight requirement as set out by ADS-33E-PRF.

Design Method and Results

Based on the analyses made earlier, a method to design the propeller of the coaxial compound helicopter is presented here. Both design parameters and the position of the propeller are taken into account. The method aims at reducing the power consumption at both the maximum speed and optimum speed ranges. Handling qualities requirements, especially the p/q coupling requirement are also considered.

According to the Adkins and Liebeck method, the lift-to-drag of the propeller airfoil is critical in the design process. Fig. 16 presents the lift-to-drag ratio of the Clark Y airfoil at different Mach numbers [35]. This airfoil has been used both in this article and the previous studies [22].

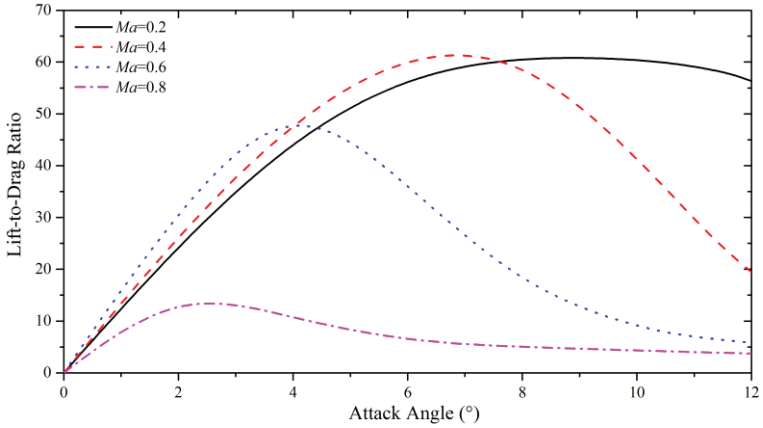

Fig. 16 Lift-to-drag ratios of airfoil at various Mach numbers

Using the Adkins-Liebeck method, the angle of attack at any radial station on the propeller disc should be the angle corresponding to the best lift-to-drag ratio. However, as demonstrated in Fig.16, the angle of attack can vary within a given range while maintaining good lift-to-drag ratio. For instance, when the Mach number is 0.2, the angle of attack corresponding to the best lift-to-drag ratio is about 8.5 degrees. However, as the lift-to-drag ratio changes only slightly around this value, the angle of attack can pick up any value between 7 degrees and 10 degrees and still maintain acceptable efficiency. This gives the design method additional freedom to adjust the chord and pre-twist distribution to acquire a relatively better performance at both the maximum and optimum speed ranges.

Meanwhile, the range of the angle of attack that maintains a reliable lift-to-drag ratio shrink as the Mach number increases. In other words, it is harder to adjust the chord and pre-twist distribution in high speed flight.

In light of the idea mentioned above, the propeller design procedure is formulated as a nonlinearly constrained optimisation problem (NCOP) to optimise the performance in high-speed flight. Further, the optimum flight speed (the speed correspondence to the maximum flight range) should also be considered.

Optimal variables

In this NCOP, the optimal variables vector $\boldsymbol{x}$ is shown in Eq. (37).

$$\boldsymbol{x}=[r_p,\Omega_p,N_b,c_p,\theta_{pretwist},Z_p] \tag{37}$$

The position parameter Y_p is excluded in this procedure and is fixed at zero to decrease the power consumption in high-speed flight and guarantee the satisfied lateral trim and controllability characteristics, based on previous analyses.

Cost function

The cost function of the NCOP is the power consumption of the coaxial compound helicopter at the forward speed of 100m/s (maximum flight speed). Hence, the cost function can be formulated into the following general expression,

$$min(J) = P_{p,v=100m/s} + P_{r,v=100m/s} \tag{38}$$

where J is the cost function; $P_{p,v=100m/s}$ and $P_{r,v=100m/s}$ are the power consumption of the propeller and the coaxial rotor at 100m/s.

Constraints

The constraint equations here are aimed to guarantee the performance at the optimum forward speed (60 m/s), to improve the handling qualities of the helicopter, and to optimise the propeller efficiency.

(1) Performance at the optimum forward speed

According to Fig. 16 and the related analysis, the power required at the optimum speed (60m/s) can be considered as a constraint of the airfoil attack angle. In other words, the angle of attack at every propeller blade element should be limited to a given range to the local Mach number to obtain a preferable airfoil lift-to-drag ratio. Thus, this constraint is formulated as follow.

$$\alpha_{l,limit} \le \alpha(r)_{v=60m/s} \le \alpha_{u,limit} \tag{39}$$

where $\alpha_{l,limit}$ and $\alpha_{u,limit}$ are the lower and upper limits of the angle of attack, which can be obtained by the airfoil aerodynamics characteristics.

(2) Handling qualities requirement

As analysed previously, the propeller parameters influence the p/q coupling. Therefore, the constraint of the coupling is shown in Eq. (40).

$$dB(p/q) < -10 \tag{40}$$

The value -10 is set based on Level 1 of the corresponding requirement in ADS-33E-PRF. In the design process, the thrust allocation factor a_{rp} in Eq. (35) is equal to 1.0 to ensure adequate inter-axis coupling handling qualities in the most critical situation.

(3) Propeller efficiency

The solidity of the propeller should not be too large so that the blade can operate at the best blade loading and reduce the profile power [36, 37]. Therefore, extra boundary condition Eq. (41) is added in terms of the solidity.

$$\sigma \le 0.4 \tag{41}$$

where σ is the solidity of the propeller.

Other constraints are formulated as follow to guarantee the propeller sufficient thrust in high speed flight and to avoid the compressibility effect at the propeller blade tips:

$$\Omega_p R_p \le M_{a,Critical} \bullet a_c \tag{42}$$

$$R_{gr,lim} - Z_p \ge R_p \ge 1.2m \tag{43}$$

$$\Omega_p \ge 148.1rad/s \tag{44}$$

$$c \ge 0.11m \tag{45}$$

where $M_{a,Critical}$ is the critical Mach number of the airfoil; c is the average chord length. The critical Mach number is obtained from the aerodynamics look-up table of the airfoil. Eqns. (43-45) are to guarantee the propeller the sufficient potential to provide the thrust needed for trimmed flight at the maximum flight range.

The design process can be further explored as the design parameters of the propeller have little influence on the flight dynamics characteristics and the power consumption of the coaxial rotors. The optimisation procedure can be divided into inner-loop NCOP and outer-loop NCOP. Fig.17 shows the flowchart of the propeller design process.

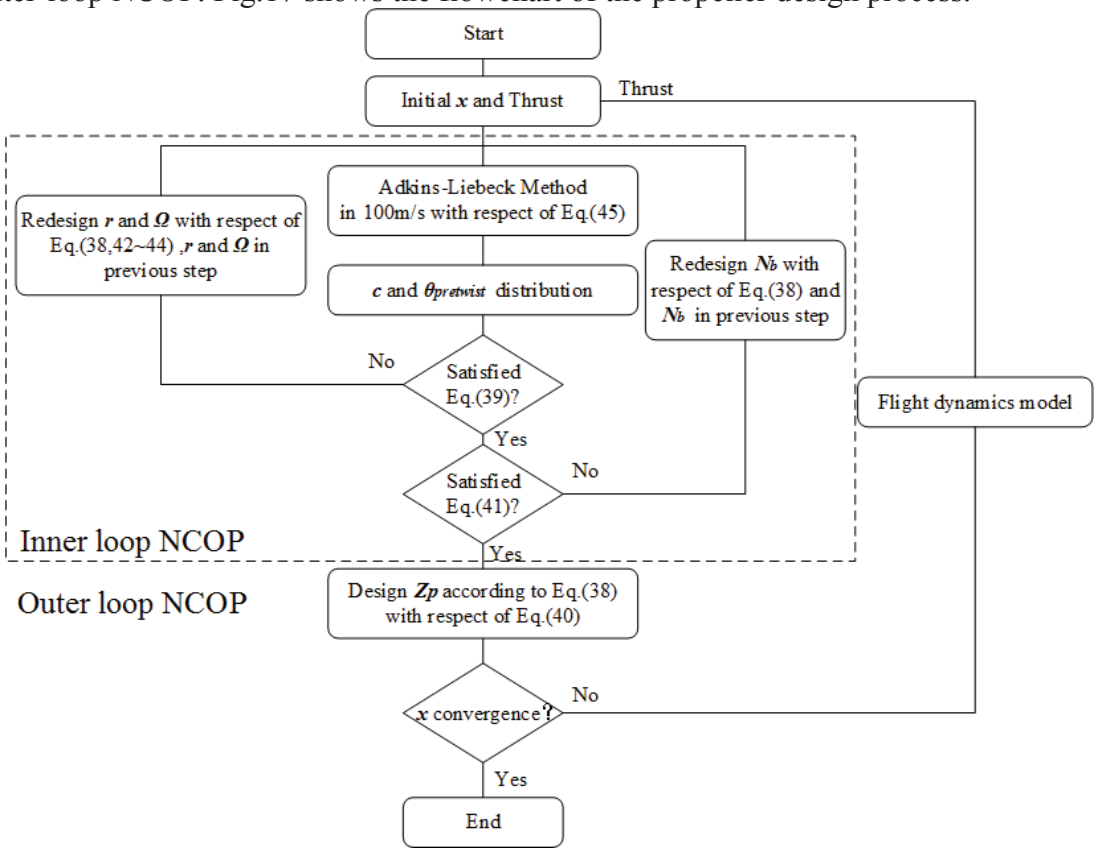

Fig. 17 Flowchart of the propeller design process

In the flowchart in Fig. 17, the design parameters are optimised in the inner loop NCOP, which is only based on the model of the propeller. The flight dynamics model of the coaxial compound helicopter is only utilised in the process of the propeller position optimisation design in outer loop NCOP.

Results

The optimal propeller parameters are shown in Table.2 and Fig. 17, along with the original is taken from Table.1.

Table. 2 The designed propeller parameters

Parameter	Original	Optimal
Propeller radius/m	1.3	1.46
Number of blades	5	6
Propeller rotational speed/(rad/s)	162	167.7
Chord length/m	0.16	In Fig. 18(a)
Pre-twist/°	30 (Linear)	In Fig. 18(b)
Coordinates of Z(m)	0.00	-1.18

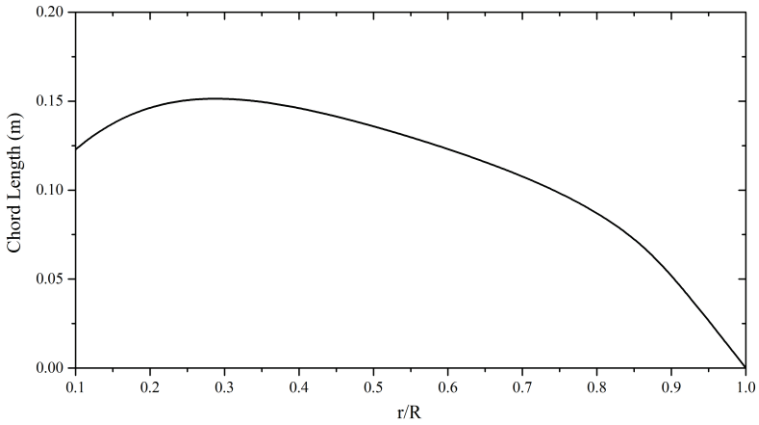

(a) Chord length

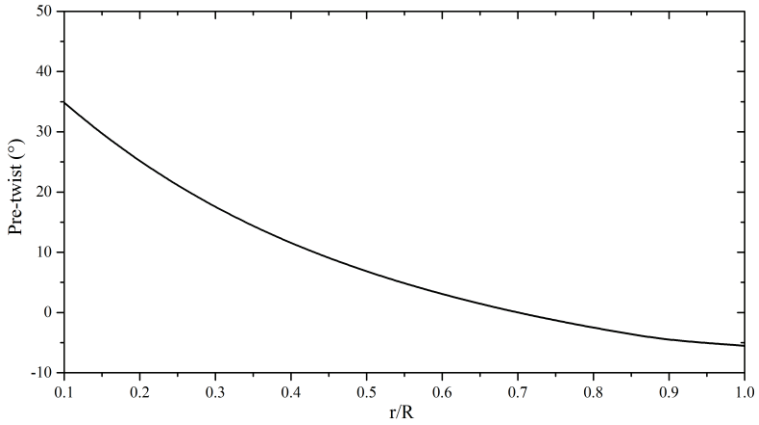

(b) Pre-twist

Fig. 18 Optimal results for chord length and the pre-twist

According to the results, the design and location parameters are changed to a large extent after the optimisation. Compared to the original results, the solidity of the propeller does not change to a large extent. Nevertheless, the average chord length is reduced based on the result of the Adkins and Liebeck method. Also, the pre-twist is altered from 30 degrees to around 40 degrees to enhance the propeller aerodynamic efficiency. Meanwhile, the blade radius and tip speed are also changed in order to strike a balance between the propulsion requirement and the aerodynamic efficiency. The tip speed of the propeller increases from 210.6 m/s to 244.8 m/s. Therefore, the dynamic pressure of the blade tip goes up so that the angle of attack of each blade element remains in their optimal incidence range. Also, the compressibility effects are automatically considered in the optimisation. When the vehicle is flying at 100 m/s, the compressibility effects are minimised as the blade tip Mach number is below 0.8, which ensures the good performance characteristics. The Z position is also changed dramatically after the optimisation. According to the analysis results, the Z position has a direct influence on the longitudinal/lateral control coupling, the increase of the Z position could lead the propeller to provide additional pitching moment when its collective pitch increases. Therefore, the relevant handling qualities requirement can be satisfied. Also, the pre-twist and chord length value after the optimisation process indicate a further performance improvement can be achieved. Altering these parameters ensure the propeller has the potential to improve the performance and flight dynamics characteristics of the coaxial compound helicopter.

Based on these optimised results, the power consumption of the propeller and the coaxial rotor and the inter-axis p/q coupling results are shown in Table.3.

Table. 3 Power required and p/q coupling results

	60m/s		100m/s	
	Power (Kw)	p/q (dB)	Power (Kw)	p/q (dB)
Original	402.8	71.5	1018.9	69.7
Optimised	389.7	-11.2	977.9	-10.3

As shown in Table.3, the optimised propeller parameters reduce the power consumption at both the optimum speed (60m/s) and the maximum speed (100m/s) ranges. Meanwhile, the average p/q inter-axis coupling can be guaranteed to satisfy the level 1 requirement of ADS-33E-PRF.

Conclusions

An overview of the Adkins-Liebeck propeller design method is first presented in this article. A model of the coaxial compound helicopter is developed to study the influence of propeller design parameters on the flight dynamics characteristics and performance of co-axial compound helicopters, and a design method for the propeller of the coaxial compound helicopter was proposed. The results of the simulation and analysis allow the following conclusion to be drawn:

1) The design propeller parameters, including the radius, propeller rotational speed, number of blades, chord, and pre-twist, have a slight influence on the trim and the handling qualities characteristics. However, they have evident effects on the propeller power consumption.

2) The position of the propeller alters the flight dynamics characteristics and power required and have a slight influence on the eigenvalues results. The Y position changes the lateral trim results, and the Z position can alter the longitudinal trim results and the average inter-axis coupling of p/q. Both Y and Z positions affect the power consumption of both the propeller and the coaxial rotor.

3) Propeller optimisation framework based on the Adkins-Liebeck method for the propeller of the coaxial compound helicopter was developed to extend the performance at optimum and maximum speed range. Additionally, the method can ensure the longitudinal to lateral inter-axis coupling meet the associated requirement in the ADS-33E-PRF handling qualities requirements.

The proposed method provides a feasible optimization method to improve the propeller aerodynamic efficiency and the associated flight dynamics and handling qualities characteristics of the coaxial compound helicopter. In the future, the aeroacoustics analysis and structural dynamics characteristics can be taken into the optimisation process to further enhance this method.

References

[1] Qi, Haotian, et al. "A study of coaxial rotor aerodynamic interaction mechanism in hover with high-efficient trim model." *Aerospace Science and Technology* 84 (2019): 1116-1130.

[2] Yeo, Hyeonsoo. "Design and aeromechanics investigation of compound helicopters." *Aerospace Science and Technology* 88 (2019): 158-173.

[3] Moodie, Alex M., and Hyeonsoo Yeo. "Design of a cruise-efficient compound helicopter." *Journal of the American Helicopter Society* 57.3 (2012): 1-11.

[4] Bagai, Ashish. "Aerodynamic design of the X2 technology demonstrator™ main rotor blade." Annual Forum Proceedings American Helicopter Society. Vol. 64. No. 1. American Helicopter Society, INC, 2008.

[5] Ferguson, Kevin, and Douglas Thomson. "Performance comparison between a conventional helicopter and com-pound helicopter configurations." *Proceedings of the Institution of Mechanical Engineers, Part G: Journal of Aerospace Engineering* 229.13 (2015): 2441-2456.

[6] Arcidiacono, Peter J., Gary deSimone, and John Occhiato. "Preliminary Evaluation of RSRA Data Comparing Pure Helicopter, Auxiliary Propulsion and Compound Helicopter Flight Characteristics." *Journal of the American Helicopter* Society 27.1 (1982): 42-51.

[7] Crossley, William A., and David H. Laananen. "Conceptual design of helicopters via genetic algorithm." *Journal of Aircraft* 33.6 (1996): 1062-1070.

[8] Sekula, Martin K., and Farhan Gandhi. "Effects of auxiliary lift and propulsion on helicopter vibration reduction and trim." *Journal of aircraft* 41.3 (2004): 645-656.

[9] Lyu, Wei-Liang, and Guo-Hua Xu. "New-Trim-Method-Based Investigation on the Cyclic-Pitch-Effected Advancing-Blade-Concept Helicopter Aerodynamics." *Journal of Aircraft* (2015), 52 (4) :1-7

[10] Ruddell, Andrew J. "Advancing blade concept (ABC™) development." *Journal of the American Helicopter Society* 22.1 (1977): 13-23.

[11] Gur, Ohad, and Aviv Rosen. "Optimising electric propulsion systems for unmanned aerial vehicles." *Journal of aircraft* 46.4 (2009): 1340.

[12] Chattot, Jean-Jacques. "Optimisation of propellers using helicoidal vortex model." *Computational Fluid Dynamics Journal* 10.4 (2002): 429-438.

[13] Morgado, J., et al. "High altitude propeller design and analysis." *Aerospace Science and Technology* 45 (2015): 398-407.

[14] Enconniere, Julien, Jesús Ortiz-Carretero, and Vassilios Pachidis. "Mission optimisation for a conceptual coaxial rotorcraft for taxi applications." *Aerospace Science and Technology* 72 (2018): 14-24.

[15] Adkins, Charles N., and Robert H. Liebeck. "Design of optimum propellers." *Journal of Propulsion and Power* 10.5 (1994): 676-682.

[16] Walsh, D., et al. "High Airspeed Testing of the Sikorsky X2 Technology TM Demonstrator." American Helicopter Society 67th Annual Forum, Virginia Beach, VA. 2011.

[17] Walsh, D., et al. "Development testing of the Sikorsky X2 technology demonstrator." American helicopter society 65th annual forum. 2009.

[18] Swartzwelder, Matthew A. Trim and control optimisation of a compound helicopter model. Diss. Pennsylvania State University, 2003 (Chapter 3).

[19] Russel, Carl, and Wayne Johnson. "Conceptual design and performance analysis for a large civil compound helicopter." Future Vertical Lift Aircraft Design Conference, American Helicopter Society Specialists meeting, San Francisco, CA, USA. 2012.

[20] Enconniere, Julien, Jesus Ortiz-Carretero, and Vassilios Pachidis. "Mission performance analysis of a conceptual coaxial rotorcraft for air taxi applications." *Aerospace Science and Technology* 69 (2017): 1-14.

[21] Hersey, Sean, Ananth Sridharan, and Roberto Celi. "Multi-objective Performance Optimisation of a Coaxial Compound Rotorcraft Configuration." Journal of Aircraft (2017), 54 (4) :1-10

[22] Ferguson, Kevin M. Towards a better understanding of the flight mechanics of compound helicopter configurations. Diss. University of Glasgow, 2015 (Chapters 2-4).

[23] Reid, Elliot G. The influence of blade-width distribution on propeller characteristics. STANFORD UNIV CA, ADA380686, 1949.

[24] Yuan, Ye, Renliang Chen, and Pan Li. "Trim investigation for coaxial rigid rotor helicopters using an improved aerodynamic interference model." *Aerospace Science and Technology* 85 (2019): 293-304.

[25] Leishman, Gordon J. Principles of helicopter aerodynamics with CD extra. Cambridge university press, 2006.

[26] Padfield, Gareth D. Helicopter flight dynamics. John Wiley & Sons, 2008 (Chapters 3 & 4).

[27] Ji, Honglei, Renliang Chen, and Pan Li. "Real-time simulation model for helicopter flight task analysis in turbulent atmospheric environment." *Aerospace Science and Technology* 92 (2019): 289-299.

[28] Phelps.A E, Mineck R E. Aerodynamic characteristics of a counter-rotating, coaxial, hingeless rotor helicopter model with auxiliary propulsion. NASA-TM-78705, May 1978.

[29] Yeo, Hyeonsoo, and Wayne Johnson. "Investigation of maximum blade loading capability of lift-offset rotors." *Journal of the American Helicopter Society* 59.1 (2014): 1-12.

[30] Cameron, Christopherl G. "Performance and Loads of a Lift Offset Rotor: Hover and Wind Tunnel Testing." *Journal of the American Helicopter Society* 64.2 (2019): 1-12.

[31] Feil, Roland, et al. "Aeromechanics Analysis of a High-Advance-Ratio Lift-Offset Coaxial Rotor System." *Journal of Aircraft* 56.1 (2018): 166-178.

[32] Rand, Omri, et al. "Lift offset: an analytical insight." *Aircraft Engineering and Aerospace Technology* 88.6 (2016): 753-760.

[33] Blackwell, R., and T. Millott. "Dynamics design characteristics of the Sikorsky X2 technology™ demonstrator aircraft." annual forum proceedings-American helicopter society. Vol. 64. No. 1. American helicopter society, INC, 2008.

[34] Standard, Aeronautical Design. "Handling Qualities Requirements for Military Rotorcraft (ADS-33E-PRF)." US Army Aviation and Missile Command, Aviation Engineering Directorate, Redstone Arsenal, Alabama, US (2000).

[35] Silverstein A. "Scale effect on Clark Y airfoil characteristics from NACA full-scale wind-tunnel tests." NACA-TR-5035. 1935

[36] Yaggy, Paul F., and Vernon L. Rogallo. "A wind-tunnel investigation of three propellers through an angle-of-attack range from 0 degree to 85 degrees." National Aeronautics and Space Administration, 1960.

[37] Wald, Quentin R. "The aerodynamics of propellers." *Progress in Aerospace Sciences* 42.2 (2006): 85-128.